Multiple virulence factors regulated by AlgU contribute to the pathogenicity of *Pseudomonas savastanoi* pv. *glycinea* in soybean

Viet Tru Nguyen [Equal first author, 1, 2] , **Nanami Sakata** [Equal first author, 2] , **Giyu Usuki** [2] , **Takako Ishiga** [2] , **Yoshiteru Hashimoto** [2, 3] , **Yasuhiro Ishiga** [Corresp. 2]

1 Western Highlands Agriculture and Forestry Science Institute, Buon Ma Thuot, Daklak, Vietnam

2 Faculty of Life and Environmental Sciences, University of Tsukuba, Tsukuba, Ibaraki, Japan

3 Microbiology Research Center for Sustainability (MiCS), University of Tsukuba, Tsukuba, Ibaraki, Japan

Corresponding Author: Yasuhiro Ishiga
Email address: ishiga.yasuhiro.km@u.tsukuba.ac.jp

Pseudomonas savastanoi pv. *glycinea* (*Psg*) causes bacterial blight of soybean. To identify candidate virulence factors, transposon-mediated mutational analysis of *Psg* was carried out. We syringe-inoculated soybean leaves with *Psg* transposon mutants and identified 28 mutants which showed reduced virulence from 1,000 mutants screened. Next, we spray-inoculated soybean leaves with these mutants and demonstrated that the *algU* mutant showed significantly reduced virulence together with reduced bacterial populations *in planta*. Expression profiles comparison between the *Psg* wild-type (WT) and *algU* mutant in HSC broth revealed that expression of coronatine (COR)-related genes (including *cmaA* and *corR*) were down-regulated in the *algU* mutant compared with *Psg* WT. Moreover, we also showed that COR production were reduced in the *algU* mutant compared with WT. We also demonstrated that *algD*, which is related to alginate biosynthesis, showed reduced expression and biofilm formation was significantly suppressed in the *algU* mutant. Furthermore, *hrpL* also showed less expression in the *algU* mutant. These results indicate that AlgU plays a critical role in promoting *Psg* pathogenesis by regulating multiple virulence factors.

1 Multiple virulence factors regulated by AlgU contribute
2 to the pathogenicity of *Pseudomonas savastanoi* pv.
3 *glycinea* in soybean

6 Viet Tru Nguyen[1,2]*, Nanami Sakata[1]*, Giyu Usuki[1], Takako Ishiga[1], Yoshiteru Hashimoto[1,3] and
7 Yasuhiro Ishiga[1]

9 [1]Faculty of Life and Environmental Sciences, University of Tsukuba, 1-1-1 Tennodai, Tsukuba,
10 Ibaraki 305-8572, Japan.
11 [2]Western Highlands Agriculture and Forestry Science Institute, 53 Nguyen Luong Bang Street,
12 Buon Ma Thuot City, Daklak Province, Vietnam.
13 [3]Microbiology Research Center for Sustainability (MiCS), University of Tsukuba, 1-1-1 Tennodai,
14 Tsukuba, Ibaraki 305-8572, Japan.

16 *These authors contributed equally to this work.

18 Corresponding Author:
19 Yasuhiro Ishiga[1]
20 1-1-1 Tennodai, Tsukuba, Ibaraki 305-8572, Japan.
21 Email address: ishiga.yasuhiro.km@u.tsukuba.ac.jp

23 Abstract

24   *Pseudomonas savastanoi* pv. *glycinea* (*Psg*) causes bacterial blight of soybean. To identify
25 candidate virulence factors, transposon-mediated mutational analysis of *Psg* was carried out. We
26 syringe-inoculated soybean leaves with *Psg* transposon mutants and identified 28 mutants which
27 showed reduced virulence from 1,000 mutants screened. Next, we spray-inoculated soybean leaves
28 with these mutants and demonstrated that the *algU* mutant showed significantly reduced virulence
29 together with reduced bacterial populations *in planta*. Expression profiles comparison between the
30 *Psg* wild-type (WT) and *algU* mutant in HSC broth revealed that expression of coronatine (COR)-
31 related genes (including *cmaA* and *corR*) were down-regulated in the *algU* mutant compared with
32 *Psg* WT. Moreover, we also showed that COR production were reduced in the *algU* mutant
33 compared with WT. We also demonstrated that *algD*, which is related to alginate biosynthesis,
34 showed reduced expression and biofilm formation was significantly suppressed in the *algU*
35 mutant. Furthermore, *hrpL* also showed less expression in the *algU* mutant. These results indicate
36 that AlgU plays a critical role in promoting *Psg* pathogenesis by regulating multiple virulence
37 factors.

39 Introduction

40   *Pseudomonas savastanoi* pv. *glycinea* (*Psg*) causes bacterial blight of soybean. The disease
41   is characterized by circular necrotic lesions on leaves surrounded by a chlorotic halo (Ignjatov et
42   al., 2007). In *P. syringae*, *P. cannabina,* and *P. savastanoi,* the phytotoxin Coronatine (COR) is
43   important in inducing chlorosis, and contributes to bacterial growth and lesion formation (Bender
44   et al., 1987; Budde and Ullrich, 2000; Peñaloza-Vázquez et al., 2000; Uppalapati et al., 2005; Qi
45   et al., 2011; Sakata et al., 2021). In *Psg* PG4180, COR synthesis genes reside on a 90 kb plasmid
46   designated p4180A (Bender et al., 1991), with a 32 kb COR gene cluster which consists of two
47   distinct regions encoding coronafacic acid (CFA) and coronamic acid (CMA) (Bender, 1999). *Psg*
48   produces COR not only for the biological fitness of pathogens in planta (Ullrich et al., 1993) but
49   also *in vitro* (Hoitink and Sinden, 1970; Palmer and Bender, 1993). Many studies showed the roles
50   of COR in chlorosis, promoting lesion formation, and suspension of both stomatal and salicylic
51   acid (SA)-dependent defenses (Peñaloza-Vázquez et al., 2000; Kloek et al., 2001; Zhao et al.,
52   2003; Brooks et al., 2005; Melotto et al., 2006; Uppalapati et al., 2007). COR contributes to *P.
53   syringae* pv. *tomato* (*Pst*) DC3000 virulence by suppressing the host defense response (Uppalapati
54   et al., 2007). COR suppresses pathogen-associated molecular pattern (PAMP)-triggered immunity
55   (PTI), especially stomatal-based defense in the early *Pst* DC3000 infection stage in *Arabidopsis
56   thaliana* and tomato (Melotto et al., 2006; Ishiga et al., 2018).

57   Besides COR, the type three secretion system (T3SS) also plays a critical role in *P. syringae*
58   virulence. The T3SS, is encoded by the *hrp* (*h*ypersensitive *r*esponse and *p*athogenicity) cluster,
59   and transfers type three effectors (T3Es) into plant cells to suppress PTI, contribute to
60   pathogenesis, and enhance disease symptoms and bacterial multiplication (Brooks et al., 2005;
61   Lam et al., 2014). Furthermore, *Psg* also produces pectolytic enzymes which allow the pathogen
62   to invade and multiply in the intercellular spaces of host tissues. This is the physiological capability
63   of *Psg* in using plant polysaccharides and providing flexibility for its pathogen activity (Haefelet
64   and Lindow, 1987).

65   AlgU, an extracytoplasmic function (ECF) sigma factor, is also important in supporting *P.
66   syringae* growth and disease development (Markel et al., 2016). AlgU regulates between 800 to
67   1,000 genes (Yu et al., 2014), and importantly contributes to virulence gene regulation as well as
68   flagellin repression (Schreiber and Desveaux, 2011; Markel et al., 2016; Bao et al., 2020). *Pst*
69   DC3000 AlgU is not only able to regulate gene expression associated with T3SEs and the
70   phytotoxin COR, but also alginate biosynthesis (Ishiga et al., 2018). Moreover, AlgU (previously
71   called AlgT) also induces transcription of the *algT-mucAB* gene cluster and the *algD* operon, which
72   are responsible for alginate biosynthesis in *Psg* PG4180 (Schenk et al., 2006). Although AlgU has
73   been extensively studied in several *P. syringae* pathovars, its roles in *Psg* pathogenicity have not
74   been elucidated yet.

75   To identify genes related to *P. syringae* pathogenicity, researchers carried out a screen for
76   *P. syringae* mutants with reduced virulence. *Pst* DC3000 Tn*5* mutants with reduced virulence on
77   *A. thaliana* found the crucial functions of COR in virulence (Brooks et al., 2004). Sakata et al.,
78   (2019) also screened for *P. cannabina* pv. *alisalensis* (*Pcal*) KB211 Tn*5* mutants with reduced
79   virulence on cabbage plants using a dip-inoculation method, and identified multiple virulence

80 factors including the T3SS, membrane transporters, transcription factors, and amino acid
81 metabolism genes. Thus, it is tempting to speculate that each *P. syringae* pathovar has developed
82 its own virulence factors. However, a screening study to identify *Psg* virulence factors has not
83 been conducted previously.

84   To investigate *Psg* virulence factors, we constructed a bacterial mutant library based on
85 transposon insertion in *Psg*, and screened for mutants with less or no chlorosis on soybean leaves
86 after syringe-inoculation. We successfully identified several virulence factors including COR,
87 T3Es, and AlgU. Expression profiles revealed that AlgU promotes virulence in host plants not
88 only by up-regulation of COR-related gene expression. We also showed that *algU* mutant showed
89 reduced COR production and biofilm formation compared to WT. Our results provide evidence
90 that AlgU plays a critical role in promoting *Psg* pathogenesis.

91

Materials & Methods

Bacterial strains, plasmids, and growth conditions

94   The bacterial strains and plasmids used in this study are listed in Table 1. *Pseudomonas*
95 strains were routinely cultured on King's B (KB; King et al., 1954) medium or mannitol-glutamate
96 (MG; Keane et al., 1970) medium at 28°C. *Escherichia coli* (*E. coli*) cultures were grown on Luria-
97 Bertani (LB; Sambrook et al. 1989) medium at 37°C. The bacterial cell densities at 600 nm (OD_{600})
98 were measured using a Biowave CO8000 Cell Density Meter (Funakoshi, Tokyo, Japan) as
99 described in Sakata et al., (2021).

100

Bacterial *in vitro* Growth Measurements

102   Wild-type, the *algU* mutant, and the *algU*-complemented strain were grown at 28°C on LB
103 medium. The bacterial suspensions were standardized to an OD_{600} of 0.05 with LB, and bacterial
104 growth was measured at OD_{600} for 6, 9, and 12 h.

105

Plant material and inoculation procedures

107   Soybean plants (*Glycine max*), cultivar "Enrei", were grown in a growth chamber at 22°C,
108 with approximately 60% humidity, and a supplementary light intensity of 200–350 $\mu mol/(m^2 sec)$
109 for a 14 h photoperiod. All soybean plants used for virulence studies were three or four-weeks-
110 old.

111   *Psg* carrying Tn*5* transposon was syringe-infiltrated into soybean leaves at an OD_{600} of 0.1
112 (5×10^7 CFU/ml) containing 0.02% Silwet L-77 (OSi Specialties Inc., Danbury, CT, USA). The
113 disease symptoms were fully developed at 6 days post inoculation (dpi) (Fig. 1A). The mutants
114 which showed different disease symptoms or virulence reduction in comparison to *Psg* WT were
115 selected.

116   For spray inoculation, bacterial suspensions were applied to observe disease symptoms on
117 whole soybean plants as described previously (Uppalapati et al. 2007). Plants were sprayed with a
118 bacterial suspension at an OD_{600} of 0.2 (1×10^8 CFU/ml) in sterile distilled water containing
119 0.025% Silwet L-77 until runoff. After inoculation, plants were transferred to growth chambers at

120 28°C with approximately 90 to 100% humidity for 24 h in the dark before maintaining plants at
121 approximately 70% humidity.
122   For syringe inoculation, bacteria were suspended at a final concentration at an OD_{600} of 0.1
123 (5×10^7 CFU/ml), 0.01 (5×10^6 CFU/ml), and 0.001(5×10^5 CFU/ml), and infiltrated with a 1-ml
124 blunt syringe into leaves. The plants were then incubated at 70-80% humidity for the rest of the
125 experimental period. Leaves were removed and photographed at 5 dpi.
126 To measure bacterial growth in soybean leaves after spray inoculation, individual second leaf pairs
127 were selected at 6 dpi, weighed and surface-sterilized in 5% H_2O_2 for 3 min, and then rinsed three
128 times with sterile water. The leaves were then homogenized, and appropriate dilutions were plated
129 on KB medium containing the appropriate antibiotics. The bacterial colony forming units (CFU)
130 were normalized as CFU/g using the total inoculated leaf mass. The population at 0 dpi was
131 estimated using leaves harvested 1 h post inoculation (hpi) without surface-sterilization. For
132 syringe-inoculation, leaf discs were harvested using a 3.5 mm-diameter cork-borer from syringe-
133 infiltrated leaf zone. The leaves were then homogenized, and appropriate dilutions were plated on
134 KB medium containing the appropriate antibiotics. The bacterial colony forming units (CFU) were
135 normalized as CFU/cm^2 using the leaf square meters. The bacterial populations were evaluated in
136 at least three independent experiments.

137 **Transposon-mediated mutagenesis and identification of mutated genes**
138   Transposon-mediated mutagenesis was carried out, as described previously (Sakata et al.
139 2019). Briefly, pBSLC1 (Sawada et al., 2018) carrying mini-Tn*5* transposon were transferred into
140 *Psg* to build a mutant library. We developed more than 1,000 individual *Psg* mutant lines. After
141 the inoculation assay, we identified the mutated genes by rescuing the transposon insertion sites
142 into an *E. coli* plasmid and sequencing (Sakata et al., 2019).
143

144 **Complementation of the *algU* mutant**
145   The *algU*-complemented strain was constructed as described in Ishiga et al., (2018). Briefly,
146 the pDSKG vector was made from pDSK519 vector (Keen et al., 1988) by replacing kanamycin
147 cassette to gentamycin. The *algU* and promoter region were transferred into the pDSKG vector
148 (Keen et al., 1988) to generate pDSKG-*algU*. The pDSKG-*algU* construct was introduced into the
149 *algU* mutant by electrophoresis to generate the complemented strain.
150

151 **Real-time quantitative RT-PCR**
152   For *Psg* gene expression profiles, data were collected as previously described in Sakata et
153 al., (2021). Specifically, bacteria were grown in HS medium optimized for COR production (HSC;
154 Palmer and Bender, 1993) for 3 and 48 h. Bacterial RNA was extracted using the ReliaPrep RNA
155 Cell Miniprep System Kit (Promega, WI, USA) according to the manufacture's protocol. Two
156 micrograms of total RNA were treated with gDNA Remover (TOYOBO, Osaka, Japan) to
157 eliminate genomic DNA, and the DNase-treated RNA was reverse transcribed using the ReverTra
158 Ace qPCR RT Master Mix (TOYOBO). The cDNA (1:10) was then used for RT-qPCR using the
159 primers shown in Supplementary Table S1 with THUNDERBIRD SYBR qPCR Mix (TOYOBO)

160   on a Thermal Cycler Dice Real Time System (TaKaRa). *Psg outer membrane lipoprotein I* (*oprI*)
161   was used to normalize gene expression.

162

163   **COR quantification by HPLC**
164   *Psg* WT, the *algU* mutant, and the *algU*-complemented strain were cultured in HSC for 7
165   days. Culture supernatant was obtained by centrifugation (12,000 × g for 5 min). Cell pellets were
166   dried at 65°C and weighed. The 500 µl of supernatants were extracted twice with 500 µl of ethyl
167   acetate and 25 µl of HCl, and the organic phase was transferred to a new microcentrifuge tube.
168   The sample was dried by centrifugal evaporator at 55°C, and the dried sample was dissolved with
169   0.05% trifluoroacetic acid (TFA)/acetonitrile (9:1, v/v). The culture supernatant was analyzed by
170   HPLC with a Shimadzu LC20A system equipped with a Symmetry C8 column (4.6 × 250 mm;
171   Waters Corporation, MA, USA) as described previously (Sakata et al. 2021).

172

173   **Hypertrophy-inducing activity assay on potato tuber tissue**
174   Potato tubers were cut from the central tuber portion to ensure samples of high uniformity.
175   After washing in tap water for 5 min, each disc was washed with sterile distilled water several
176   times. Potato tuber discs were inoculated using toothpicks by placing the tip in *Psg* WT, COR-
177   defective mutants (*cfa6* and *cmaA*), the *algU* mutant, and the *algU*-complemented strain on a KB
178   medium plate, and then placing the toothpick on the potato tuber disc. The discs were then placed
179   at 23°C incubator (darkness) for 5 days. Photographs were taken at 5 dpi.

180

181   **Biofilm formation assay**
182   Biofilm formation was assayed as described previously (Shao et al., 2019). Briefly, the
183   bacterial strains were incubated overnight in LB broth and resuspended in fresh LB broth to an
184   OD_{600} of 0.1. Bacterial suspensions (120 µl) were put into 96-well plates and incubated at 28°C
185   for 24, 48, 72, and 96 h. The bacterial solutions were discarded and washed three times with
186   distilled water. The biofilm forming bacteria were treated with 150 µl of 0.1% crystal violet (CV;
187   Fujifilm, Tokyo, Japan) for 20 min without shaking. The dye was discarded and washed twice with
188   distilled water. The plate was dried completely, subsequently the biofilm was eluted with 150 µl
189   of 100% ethanol, and the CV were dissolved completely. Finally, the eluted biofilm sample's
190   absorbance was measured at OD_{595}.

191

192   ## Results

193   **Identification and characterization of reduced virulence mutants**
194   To identify *Psg* virulence genes, we screened 1,000 transposon insertion mutants for reduced
195   disease symptoms on soybean leaves using the syringe-infiltration method. Disease symptoms
196   caused by *Psg* WT showed a small water-soaked lesion surrounded by regions of chlorosis (Fig.
197   1A). A total of 28 mutants showed no or less chlorosis at 6 dpi (Fig. 1B). Seventeen mutants out
198   of 28 had transposon insertions in genes encoding COR biosynthesis-related genes (Table 1).
199   Soybean leaves inoculated with COR biosynthesis mutants (VTD29, VTE13, VTI15, and VTR4),

200   the *algU* mutant (VTO41), and an unknown-function mutant (VTF6) showed no chlorosis (Fig.
201   1B).
202
203   **Reduced disease symptoms and bacterial growth in soybean**
204   We identified the 28 mutants which showed reduced disease symptoms compared to *Psg*
205   WT by syringe-inoculation (Fig. 1B). We further investigated whether these mutants also showed
206   reduced virulence via spray-inoculation, and selected 2 mutants related to COR biosynthesis
207   (*cmaA* and *cfa6*), and others. Soybean leaves inoculated with all mutants showed significantly
208   reduced bacterial populations than those of *Psg* WT (Fig. 2A). Among all mutants, the *algU* mutant
209   (VTO41) showed dramatically reduced bacterial populations and disease symptoms at 6 dpi (Figs. 2A
210   and 2B). To confirm whether the altered *algU* mutant phenotype originates from a corresponding
211   mutation, an *algU*-complemented strain was generated. *Psg* WT and the *algU*-complemented
212   strain showed the same bacterial population levels as well as disease symptom development in
213   soybean (Supplementary Figs. S1A and S1B). We also confirmed that *algU* is apparently
214   dispensable for *Psg* growth in rich LB medium, since no growth difference was observed among
215   WT, *algU* mutant, and *algU*-complemented strain (Supplementary Fig. S2).
216   To further investigate the algU contribution to *Psg* virulence, we conducted syringe infiltration
217   with WT, *algU* mutant, and *algU*-complemented strain. As a result, the *algU* mutant showed
218   reduced symptoms and bacterial populations at all inoculum levels we tested (Figs. 3A–3F). Taken
219   together, these results indicate that AlgU contributes to growth both on leaf surface and in apoplast,
220   and to causing disease.
221
222   **AlgU regulates the expression of *Psg* virulence genes in HSC medium**
223   *Pst* DC3000 AlgU positively regulates virulence gene transcription (Markel et al. 2016;
224   Ishiga et al. 2018). To investigate whether *Psg* AlgU also regulates virulence genes, we analyzed
225   virulence gene expression profiles in HSC medium. COR biosynthesis-related genes including
226   *cmaA* and *corR*, in the *algU* mutant showed reduced expression at 48 h after incubation (Figs. 4A
227   and 4C). Moreover, *hrpL*, encoding HrpL (an alternative sigma factor recognizing the *hrp* box in
228   the promoter of T3SS genes), also showed significantly less expression in the *algU* mutant at both
229   3 and 48 h after incubation compared to *Psg* WT (Fig. 4D). These results indicate that AlgU
230   positively regulates COR biosynthesis-related genes and *hrpL*.
231   To investigate whether AlgU can coordinate gene expression involved in *Psg* motility, we
232   determined the expression profile of *fliC* (encoding flagellin, relating to flagellar mobility). At 3 h
233   after incubation, there was no difference in the flagellar-encoding gene expression between the
234   *algU* mutant and *Psg* WT. However, after 48 h incubation, relative *fliC* expression was greater in
235   the *algU* mutant compared to *Psg* WT (Fig. 4E). Additionally, *algD* expression was down
236   regulated in the *algU* mutant (Fig. 4F), indicating that AlgU positively regulates alginate
237   biosynthesis-related genes.
238
239   **AlgU contributes to COR biosynthesis and biofilm formation in *Psg***

240   We demonstrated that COR biosynthesis-related genes in the *algU* mutant showed reduced
241   expression in HSC medium (Figs. 4A–4D). To investigate whether AlgU contributes to COR
242   production, we first conducted a hypertrophy-inducting activity test on potato tuber tissues for
243   COR detection (Sakai et al., 1979; Völksch et al., 1989). Potato tuber tissues inoculated with *Psg*
244   WT showed hypertrophy response, but those inoculated with COR-defective mutants (*cmaA* and
245   *cfa6*) showed no response (Fig. 5A). The *algU* mutant-inoculated potato tuber tissues showed less
246   hypertrophy response compared to those inoculated with *Psg* WT and the reduction was restored
247   in the *algU*-complemented strain (Fig. 5A). Furthermore, we also quantified COR production by
248   using HPLC. *Psg* WT produced around 90 ng/g of COR in HSC medium (Fig. 5B). However, the
249   *algU* mutant produced only around one third as much COR compared to *Psg* WT (Fig. 5B). We
250   also confirmed that the *algU*-complemented strain recovered COR production more than WT (Fig.
251   5B). Taken together, these results suggest that AlgU contributes to COR biosynthesis in *Psg*.
252   Since we also demonstrated that alginate biosynthesis-related genes *algD* showed reduced
253   expression in *algU* mutant (Fig. 4F), we next investigated the biofilm formation ability in *Psg* WT
254   and the *algU* mutant. The *algU* mutant showed a reduction in biofilm formation at 24, 48, and 72
255   hpi (Fig. 6). These results suggest that AlgU also contributes to biofilm formation in *Psg*.
256

Discussion

258   We attempted to identify *Psg* virulence factors that are crucial in soybean pathogenicity. We
259   screened 1,000 *Psg* mutants by syringe-infiltration and identified 28 mutants with reduced
260   virulence (Fig. 1B). Several important virulence factors contribute to *Psg* virulence including
261   COR, the T3SS, and AlgU (Table 1). Sigma factor AlgU regulates not only *algD*, but also other
262   virulence genes including *hrpL* and COR (Figs. 4A–4F). Our study provides new insights into
263   AlgU function as a global regulatory hub for *Psg* pathogenicity by regulating the expression of
264   multiple virulence genes.
265   Our screening identified that 17 out of 28 reduced virulence mutants were related to COR
266   biosynthesis genes. These COR biosynthesis mutants were mostly disrupted by Tn*5* on the *cfa* and
267   *cma* operons (Table 1). The *cfa* and *cma* operons encode enzymes related to CFA and CMA
268   biosynthesis, respectively, the two elements that are ligated together to form COR (Bender et al.,
269   1999). Together, these results indicate that COR is an important *Psg* virulence factor.
270   The *algU* mutant showed reduced virulence in plants both spray- and syringe-inoculated
271   (Figs. 2; Supplementary Fig. S1; Figs. 3), indicating that AlgU contributes to *Psg* multiplication
272   both on leaf surface and in apoplast, and causing disease. Our results indicate that AlgU regulate
273   several virulence factors. Firstly, gene expression related to COR biosynthesis, such as *cmaA* and
274   *corR* (but not *cfl*) were suppressed in the *algU* mutant (Figs. 4A–4C). Moreover, COR production
275   in the *algU* mutant also less than that of *Psg* WT (Figs. 5A and 5B), suggesting that AlgU
276   contributes to COR production in *Psg*. Consistent with our results, Ishiga et al. (2018)
277   demonstrated that gene expression related to COR biosynthesis was suppressed during *Pst*
278   DC3000 *algU* mutant infection. Furthermore, AlgU also contributes to *Pst* DC3000 virulence by
279   regulating COR production to overcome stomatal-based defense (Ishiga et al., 2018). Together,

280   these results suggest that AlgU suppresses stomatal-based defense in the early *Psg* infection stage
281   with soybean plants. Moreover, COR contributes to virulence by overcoming apoplastic defense
282   as well as stomatal-based defense in *Pcal* (Sakata et al., 2021). Further study on COR contribution
283   in *Psg* virulence will be needed to understand AlgU-mediated COR regulation.
284   Secondary, the *algD* expression profile in the *algU* mutant was significantly reduced in
285   comparison with *Psg* WT, indicating that AlgU is important in regulating alginate biosynthesis
286   gene expression (Fig. 4F). This result was consistent with a previous report in *Pst* DC3000
287   (Ishiga et al., 2018), in which *algD* expression was significantly suppressed in an *algU* mutant.
288   Further, alginate plays a crucial role in epiphytic fitness and survival, and contributes to *P.*
289   *syringae* virulence (Yu et al., 1999). Alginate is one of the exopolysaccharides (EPSs), which
290   are the major components of biofilms, in *Psg* (Osman et al., 1986; Sutherland, 2001). We
291   demonstrated that biofilm formation was significantly decreased in the *algU* mutant compared
292   with *Psg* WT (Fig. 6). *Psg* PG4180 AlgU is important in virulence and bacterial growth in host
293   plants, but it is not dependent on alginate production (Schenk et al., 2008; Yu et al., 2014).
294   Additionally, AlgU, but not AlgD plays a crucial role in *Pst* DC3000 virulence (Markel et al.
295   2016). Together, it is tempting to speculate that alginate function in virulence differs in each *P.*
296   *syringae* pathovar. Thus, further study is needed to understand AlgU regulating genes involved
297   in biofilm formation and alginate function in *Psg* virulence.
298   Thirdly, expression profiles also revealed *hrpL* transcripts were suppressed in the *algU*
299   mutant compared with *Psg* WT (Fig. 4D). *Pst* DC3000 AlgU functions to regulate *hrpL*
300   expression (Ishiga et al., 2018). Markel et al., (2016) also demonstrated that AlgU plays an
301   important role in virulence by regulating the expression of T3Es and *hrpL*. In *P. syringae*, both
302   the T3SS and T3Es genes are in turn encoded by the *hrp* gene cluster, while the sigma factor
303   HrpL directly regulates both *hrc* and *hop* genes (Lam et al., 2014). Although many studies were
304   caried out to elucidate the functions and mode of actions of the T3SS and its T3Es, AlgU
305   regulation on the T3SS system is still unknown in *P. syringae* infection processes. Therefore,
306   further precise characterization of AlgU-mediated T3SS regulation will be needed to understand
307   global gene expression networks during *Psg* infection.
308   Lastly, *fliC* transcripts in the *algU* mutant were increased compared with those of *Psg* WT
309   (Fig. 4E). In *Pst* DC3000, AlgU not only downregulates flagellar and chemotaxis genes *in vitro*
310   (Markel et al., 2016), but also negatively regulates *fliC* expression during infection (Bao et al.,
311   2020). *fliC* encodes the flagellin protein including the flg22 epitope which triggers PTI (Felix et
312   al., 1999; Zipfel et al., 2004; Parys et al., 2021; Colaianni et al., 2021). Recent studies reported
313   the important role of AlgU in de-flagellation during the *P. syringae*-plant interaction to reduce PTI
314   activation, and promote bacterial fitness in its host (Bao et al., 2020). Likewise, AlgU also plays
315   an important role in de-flagellation of *P. syringae* pv. *maculicula* ES4236, in which transposon
316   inactivation of AlgW led to decreased AlgU activity and increased the flagella expression, as
317   well as reduced bacterial growth *in planta* (Schreiber and Desveaux, 2011). Therefore, it is
318   tempting to speculate that high levels of flagellin protein production in the *algU* mutant activate
319   PTI.

320

Conclusions

322   Our findings indicate that multiple virulence factors regulated by AlgU, including COR
323 biosynthesis, biofilm formation, and T3SS, contributes to *Psg* virulence in soybean. Our findings
324 help to expand understanding of AlgU roles in *Psg* virulence. Further studies on AlgU regulated
325 mechanisms will be needed to fully understand *Psg* virulence.

326

Acknowledgements

328 We thank Dr. Christina Baker for editing the manuscript. *Psg* WT were given from the NARO
329 Genebank, Ibaraki, Japan.

330

References

332 Bao Z, Wei HL, Ma X, Swingle B (2020) *Pseudomonas syringae* AlgU downregulates flagellin
333   gene expression, helping evade plant immunity. J Bacteriol 202:e00418–19
334 Bender CL (1999) Chlorosis-inducing phytotoxins produced by *Pseudomonas syringae*. Eur J
335   Plant Pathol 105:1–12
336 Bender CL, Young SA, Mitchell RE (1991) Conservation of plasmid DNA sequences in
337   coronatine-producing pathovars of *Pseudomonas syringae*. Appl Environ Microbiol 57:993–
338   999
339 Bender CL, Srone HE, Sims JJ, Cooksey DA (1987) Reduced pathogen fitness of *Pseudomonas*
340   *syringae* pv. *tomato* Tn*5* mutants defective in coronatine production. Physiol Mol Plant
341   Pathol 30:237–283
342 Brooks DM, Bender CL, Kunkel BN (2005) The *Pseudomonas syringae* phytotoxin coronatine
343   promotes virulence by overcoming salicylic acid-dependent defenses in *Arabidopsis*
344   *thaliana*. Mol Plant Pathol 6:629–639
345 Brooks DM, Hernández-Guzmán G, Kloek AP, Alarcón-Chaidez F, Sreedharan A, Rangaswamy
346   V, Peñaloza-Vázquez A, Bender CL, Kunkel BN (2004) Identification and characterization
347   of a well-defined series of coronatine biosynthetic mutants of *Pseudomonas syringae* pv.
348   *tomato* DC3000. Mol Plant Microbe Interact 17:162–174
349 Budde IP, Ullrich MS (2000) Interactions of *Pseudomonas syringae* pv. *glycinea* with host and
350   nonhost plants in relation to temperature and phytotoxin synthesis. Mol Plant Microbe
351   Interact 13:951–61
352 Colaianni NR, Parys K, Lee H-S, Conway JM, Kim NH, Edelbacher N, Mucyn TS, Madalinski
353   M, Law TF, Jones CD, Belkhadir Y, Dangl JL (2021) A complex immune response to
354   flagellin epitope variation in commensal communities. Cell Host Microbe 29:635–649.e9
355 Felix G, Duran JD, Volko S, Boller T (1999) Plants have a sensitive perception system for the
356   most conserved domain of bacterial flagellin. Plant J 18:265–276
357 Haefelet DM, Lindow SE (1987) Flagellar motility confers epiphytic fitness advantages upon
358   *Pseudomonas syringae*. Appl Environ Microbiol 53:2528–2533

359   Hoitink H, and Sinden S (1970) Partial purification and properties of chlorosis inducing toxins of
360   *Pseudomonas phaseolicola* and *Pseudomonas glycinea*. Phytopathology 60:1236–1237

361   Ignjatov M, Milošević M, Nikolić Z, Vujaković M, Petrović D (2007) Characterization of
362   *Pseudomonas savastanoi* pv. *glycinea* isolates from Vojvodina. The Polish Phytopathol
363   Soci 45:43–54

364   Ishiga T, Ishiga Y, Betsuyaku S, Nomura N (2018) AlgU contributes to the virulence of
365   *Pseudomonas syringae* pv. *tomato* DC3000 by regulating production of the phytotoxin
366   coronatine. J Gen Plant Pathol 84:189–201

367   Keane P, Kerr A, New P (1970) Crown gall of stone fruit II. Identification and nomenclature of
368   Agrobacterium isolates. Aust J Biol Sci 23:585–596

369   Keen NT, Tamaki S, Kobayashi D, Trollinger D (1988) Improved broad-host-range plasmids for
370   DNA cloning in gram-negative bacteria. Gene 70:191–197

371   King EO, Ward MK, Raney DE (1954) Two simple media for the demonstration of pyocyanin
372   and fluorescin. J Lab Clin Med 44:301–307

373   Kloek AP, Verbsky ML, Sharma SB, Schoelz JE, Vogel J, Klessig DF, Kunkel BN (2001)
374   Resistance to *Pseudomonas syringae* conferred by an *Arabidopsis thaliana coronatine-*
375   *insensitive* (*coi1*) mutation occurs through two distinct mechanisms. Plant J 26:509–522

376   Lam HN, Chakravarthy S, Wei HL, Nguyen BH, Stodghill PV, Collmer A, Swingle BM,
377   Cartinhour SW (2014) Global analysis of the HrpL regulon in the plant pathogen
378   *Pseudomonas syringae* pv. *tomato* DC3000 reveals new regulon members with diverse
379   functions. PLoS One 9:e106115

380   Markel E, Stodghill P, Bao Z, Myers C, Swingle B (2016) AlgU controls expression of virulence
381   genes in *Pseudomonas syringae* pv. *tomato* DC3000. J Bacteriol 198:2330–2344

382   Melotto M, Underwood W, Koczan J, Nomura K, He SY (2006) Plant stomata function in innate
383   immunity against bacterial invasion. Cell 126:969–980

384   Osman SF, Fett WF, Fishman ML (1986) Exopolysaccharides of the phytopathogen
385   Pseudomonas syringae pv. glycinea. J Bacteriol 166:66–71

386   Palmer DA, Bender CL (1993) Effects of environmental and nutritional factors on production of
387   the polyketide phytotoxin coronatine by *Pseudomonas syringae* pv. *glycinea*. Appl Environ
388   Microbiol 59:1619–1626

389   Parys K, Colaianni NR, Lee H-S, Hohmann U, Edelbacher N, Trgovcevic A, Blahovska Z, Lee
390   D, Mechtler A, Muhari-Portik Z, Madalinski M, Schandry N, Rodríguez-Arévalo I, Becker
391   C, Sonnleitner E, Korte A, Bläsi U, Geldner N, Hothorn M, Jones CD, Dangl JL, Belkhadir
392   Y (2021) Signatures of antagonistic pleiotropy in a bacterial flagellin epitope. *Cell host &*
393   *microbe*.

394   Peñaloza-Vázquez A, Preston GM, Collmer A, Bender CL (2000). Regulatory interactions
395   between the Hrp type III protein secretion system and coronatine biosynthesis in
396   *Pseudomonas syringae* pv. *tomato* DC3000. Microbiology 146:2447–2456

397   Qi M, Wang D, Bradley CA, Zhao Y (2011) Genome sequence analyses of *Pseudomonas*
398   *savastanoi* pv. *glycinea* and subtractive hybridization-based comparative genomics with nine
399   Pseudomonads. PLoS One 6:e16451

400 Sakai R, Nishiyama K, Ichihara A, Shiraishi K, Sakamura S (1979) Studies on the mechanism of
401   physiological activity of coronatine. Jpn J Phytopathol 45:645–653
402 Sakata N, Ishiga T, Saito H, Nguyen VT, Ishiga Y (2019) Transposon mutagenesis reveals
403   *Pseudomonas cannabina* pv. *alisalensis* optimizes its virulence factors for pathogenicity on
404   different hosts. PeerJ 7:e7698
405 Sakata N, Ishiga T, Masuo S, Hashimoto Y, Ishiga Y (2021) Coronatine contributes to
406   *Pseudomonas cannabina* pv. *alisalensis* virulence by overcoming both stomatal and
407   apoplastic defenses in dicot and monocot plants. Mol Plant Microbe Interact doi:
408   10.1094/MPMI-09-20-0261-R
409 Sambrook J, Fritsch E, Maniatis T (1989) Molecular cloning: a laboratory manual, 2nd edition.
410   Cold Spring Harbor Laboratory, Cold Spring Harbor, New York
411 Sawada T, Eguchi M, Asaki S, Kashiwagi R, Shimomura K, Taguchi F, Matsui H, Yamamoto
412   M, Noutoshi Y, Toyoda K, Ichinose Y (2018) MexEF-OprN multidrug efflux pump
413   transporter negatively controls N-acyl-homoserine lactone accumulation in *Pseudomonas*
414   *syringae* pv. *tabaci* 6605. Mol Genet Genom 293:907–917
415 Schäfer A, Tauch A, Jäger W, Kalinowski J, Thierbach G, Pühler A. (1994) Small mobilizable
416   multi-purpose cloning vectors derived from the *Escherichia coli* plasmids pK18 and pK19:
417   selection of defined deletions in the chromosome of *Corynebacterium glutamicum*. Gene
418   145:69–73
419 Schenk A, Weingart H, Ullrich MS (2008) The alternative sigma factor AlgT, but not alginate
420   synthesis, promotes in planta multiplication of *Pseudomonas syringae* pv. *glycinea*.
421   Microbiology 154:413–421
422 Schenk A, Berger M, Keith LM, Bender CL, Muskhelishvili G, Ullrich MS (2006). The *algT*
423   gene of *Pseudomonas syringae* pv. *glycinea* and new insights into the transcriptional
424   organization of the *algT-muc* gene cluster. J Bacteriol 188:8013–8021
425 Schreiber KJ, Desveaux D (2011) AlgW regulates multiple *Pseudomonas syringae* virulence
426   strategies. Mol Microbiol 80:364–377
427 Shao X, Xie Y, Zhang Y, Deng X (2019) Biofilm formation assay in *Pseudomonas syringae*.
428   Bio-protocol 9:e3237–3237
429 Sutherland, I. (2001) Biofilm exopolysaccharides: a strong and sticky framework. Microbiology
430   147:3–9
431 Ullrich M, Bereswill S, Volksch B, Fritsche W, Geider K (1993) Molecular characterization of
432   field isolates of *Pseudomonas syringae* pv. *glycinea* differing in coronatine production.
433   Microbiology 139:1927–1937
434 Uppalapati SR, Ayoubi P, Weng H, Palmer DA, Mitchell RE, Jones W, Bender CL (2005) The
435   phytotoxin coronatine and methyl jasmonate impact multiple phytohormone pathways in
436   tomato. Plant J 42:201–217
437 Uppalapati SR, Ishiga Y, Wangdi T, Kunkel BN, Anand A, Mysore KS, Bender CL (2007) The
438   phytotoxin coronatine contributes to pathogen fitness and is required for suppression of

439   salicylic acid accumulation in tomato inoculated with *Pseudomonas syringae* pv. *tomato*
440   DC3000. Mol Plant Microbe Interact 20:955–965

441   Völksch B, Bublitz F, Fritsche W (1989) Coronatine production by *Pseudomonas syringae*
442   pathovars: screening method and capacity of product formation. J Basic Microbiol 29:463–
443   468

444   Yu J, Peñaloza-Vázquez A, Chakrabarty AM, Bender CL (1999) Involvement of the
445   exopolysaccharide alginate in the virulence and epiphytic fitness of *Pseudomonas syringae*
446   pv. *syringae*. Mol Microbiol 33:712–720

447   Yu X, Lund SP, Greenwald JW, Records AH, Scott RA, Nettleton D, Lindow SE, Gross DC,
448   Beattie GA (2014) Transcriptional analysis of the global regulatory networks active in
449   *Pseudomonas syringae* during leaf colonization. mBio 5:e01683–14

450   Zhao Y, Thilmony R, Bender CL, Schaller A, He SY, Howe GA (2003) Virulence systems of
451   *Pseudomonas syringae* pv. *tomato* promote bacterial speck disease in tomato by targeting the
452   jasmonate signaling pathway. Plant J 36:485–499

453   Zipfel C, Robatzek S, Navarro L, Oakeley EJ, Jones JDG, Felix G, Boller T (2004) Bacterial
454   disease resistance in Arabidopsis through flagellin perception. Nature 428:764–767

Bacterial strains and plasmids used in this study

Table 1 Bacterial strains and plasmid used in this study

Bacterial strain or plasmid	Locus	Relevant characteristics	Reference or source
E. coli strain			
DH5α		F−λ−φ80dLacZΔM15Δ(lacZYA-argF)U169 recA1 endA1 hsdR17 (rK−mK+) supE44 thi-1gyrA relA1	Takara, Kyoto, Japan
S17-1		Thi pro hsdR-hsdM + recA [chr::RP4-2-Tc::Km::Tn7]	Schäfer et al. 1994
P. savastanoi pv. *glycinea*			
Psg		*Psg* wild-type	MAFF301684
VTB8	PsgB076_27735	*cfa6::mTn5,* Nal^r, Km^r	This study
VTC23	PsgB076_27795	*cmaA::mTn5,* Nal^r, Km^r	This study
VTD16	PsgB076_27730	*cfa5::mTn5,* Nal^r, Km^r	This study
VTD28	PsgB076_27725	*cfa4::mTn5,* Nal^r, Km^r	This study
VTD29	PsgB076_27740	*cfa7::mTn5,* Nal^r, Km^r	This study
VTD30	PsgB076_27720	*cfa3::mTn5,* Nal^r, Km^r	This study
VTE13	PsgB076_27750	*cfa8::mTn5,* Nal^r, Km^r	This study
VTE17	PsgB076_27740	*cfa7::mTn5,* Nal^r, Km^r	This study
VTF3	PsgB076_27705	*cfa2::mTn5,* Nal^r, Km^r	This study
VTG22	PsgB076_27735	*cfa6::mTn5,* Nal^r, Km^r	This study
VTG29	PsgB076_27740	*cfa7::mTn5,* Nal^r, Km^r	This study
VTG41	PsgB076_27725	*cfa5::mTn5,* Nal^r, Km^r	This study
VTH39	PsgB076_27735	*cfa6::mTn5,* Nal^r, Km^r	This study

VTI15	PsgB076_27740	*cfa7::mTn5,* Nal^r, Km^r	This study
VTR4	PsgB076_27740	*cfa7::mTn5,* Nal^r, Km^r	This study
VTT14	PsgB076_27805	*cmaC::mTn5,* Nal^r, Km^r	This study
VTT22	PsgB076_27730	*cfa5::mTn5,* Nal^r, Km^r	This study
VTB2	PsgB076_28870	*Type III effector protein XopAD::mTn5,* Nal^r, Km^r	This study
VTB52	PsgB076_09885	*Heat shock protein 90 (Hsp90)::mTn5,* Nal^r, Km^r	This study
VTH40	PsgB076_15537	*MFS transporter::mTn5,* Nal^r, Km^r	This study
VTM22	PsgB076_27425	*Hypothetical protein::mTn5,* Nal^r, Km^r	This study
VTO15	PsgB076_01129	*ABC transporter permease::mTn5,* Nal^r, Km^r	This study
VTO41	PsgB076_06035	*Sigma factor algU::mTn5,* Nal^r, Km^r	This study
VTP20	PsgB076_26940	*DNA-binding protein::mTn5,* Nal^r, Km^r	This study
VTE41	PsgB076_09720	*Unknown,* Nal^r, Km^r	This study
VTF6	PsgB076_10315	*Unknown,* Nal^r, Km^r	This study
VTO37	PsgB076_19532	*Unknown,* Nal^r, Km^r	This study
VTT8	PsgB076_26618	*Unknown,* Nal^r, Km^r	This study
algU mutant (VTO41) + pDSKG-*algU*		*algU* mutant complemented with pDSKG-*algU*, Nal^r, Gen^r, Km^r	This study
Plasmid			
pBSLC1		Transposon vector constructed by ligation of pBSL118 and pHSG396 at EcoRI site, Amp^r, Km^r, Cm^r	Sawada et al. 2018
pDSK519		Broad-host-range cloning vector, Ken^r	Keen et al. 1998
pDSKG		Broad-host-range cloning vector, Gen^r	This study

pDSKG-*algU*	The vector containing *algU* gene inserted into pDSK519, Gen^r	This study

Notes   Amp^r ampicillin resistance, Cm^r chloramphenicol resistance, Gen^r gentamicin,

Km^r kanamycin resistance, Nal^r nalidixic acid resistance.

Figure 1

Disease symptoms on soybean leaves syringe-inoculated with *Pseudomonas savastanoi* pv. *glycinea* (*Psg*) wild-type (WT) and mutants.

(A) Disease symptoms on soybean leaves syringe-inoculated with 5×10^7 colony forming units (CFU)/ml of the *Psg* WT at 6 dpi. (B) Disease symptoms on soybean leaves syringe-inoculated with 5×10^7 colony forming units (CFU)/ml of the *Psg* mutants at 6 dpi. Scale bars shows 1 cm.

A

Psg WT

B

VTB8	VTC23	VTD16	VTD28	VTD29	VTD30	VTE13
VTE17	VTF3	VTG22	VTG29	VTG41	VTH39	VTI15
VTR4	VTT14	VTT22	VTB2	VTB52	VTH40	VTM22
VTO15	VTO41	VTP20	VTE41	VTF6	VTO37	VTT8
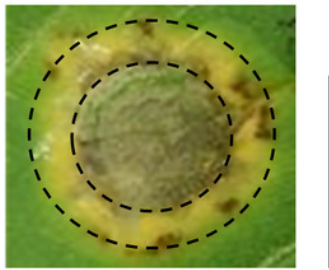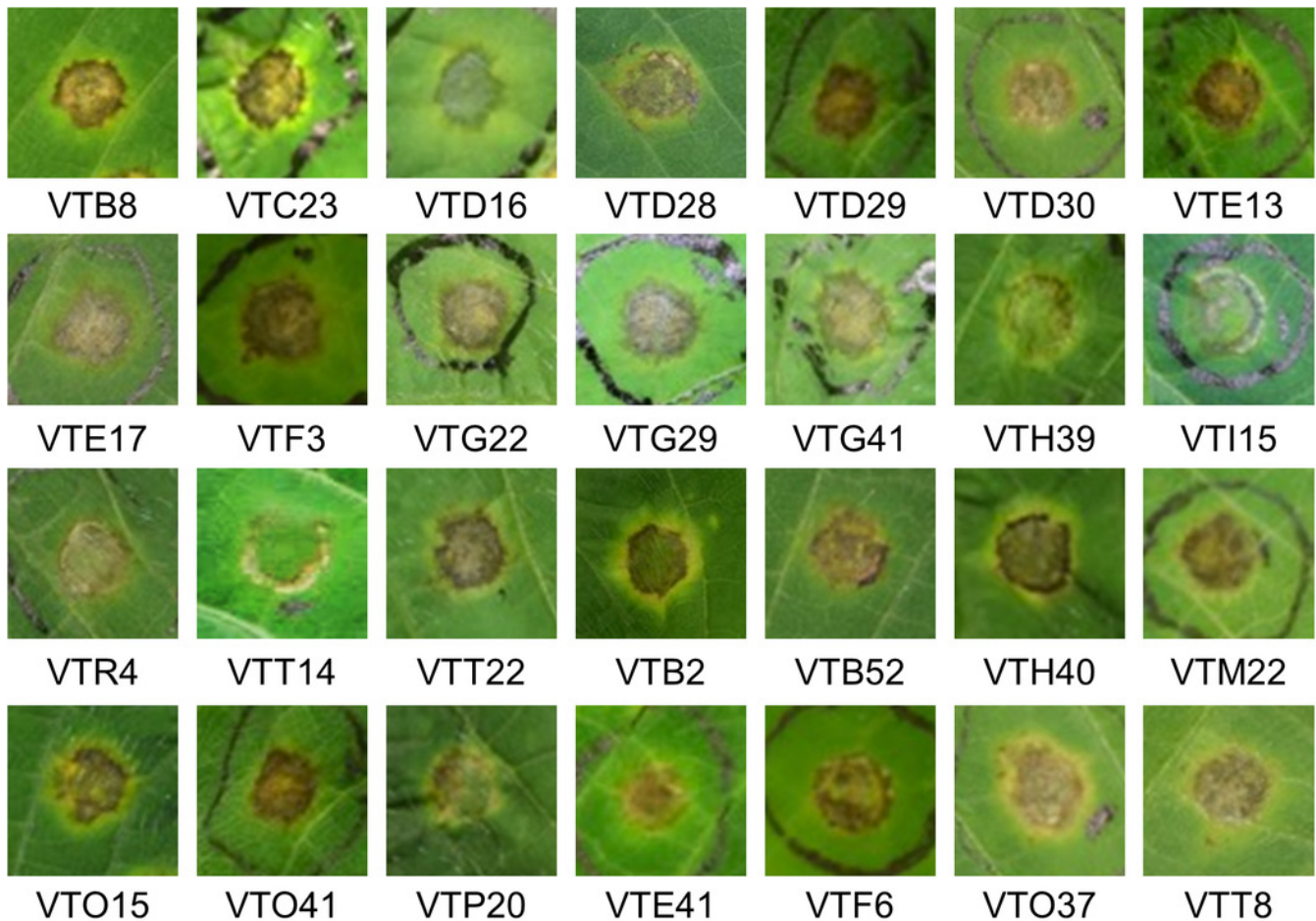
Figure 2

Bacterial populations and disease symptoms in soybean leaves.

(A) Bacterial populations in leaves spray-inoculated with *Pseudomonas savastanoi* pv.

glycinea (*Psg*) wild-type (WT) and mutants (1×10^8 colony forming units (CFU)/ml). Bacterial

populations in leaves were estimated at 6 days post inoculation (dpi) by dilution plating on

selective medium as described in the methods. Vertical bars indicate standard error for three

independent experiments. Asterisks indicate a significant difference from WT in a *t* test (*$P <$

0.05; **$P < 0.01$). (B) Disease symptoms in leaves spray-inoculated with the *Psg* WT and the

algU mutant (1×10^8 colony forming units (CFU)/ml) at 6 dpi.
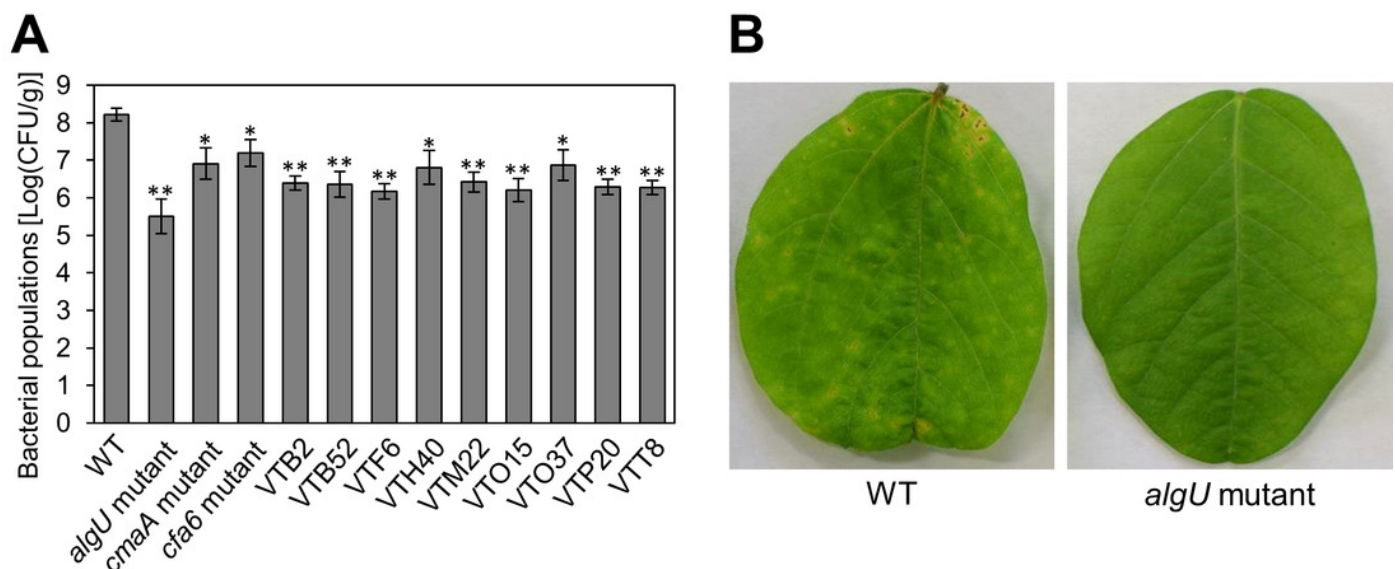
Figure 3

Disease symptoms and bacterial populations in soybean leaves after syringe inoculation.

Disease symptom and bacterial populations in leaves syringe-inoculated with *Pseudomonas syringae* pv. *glycinea* (*Psg*) wild-type (WT), the *algU* mutant, and the *algU*-complemented strain at 5×10^7 colony forming units (CFU)/ml (A, B), 5×10^6 CFU/ml (C, D), and 5×10^5 CFU/ml (E, F), respectively. Photographs were taken at 5 days post inoculation (dpi). Scale bars shows 1 cm. Bacterial populations in leaves were estimated at 5 dpi by dilution plating on selective medium as described in the methods. Vertical bars indicate standard error for three independent experiments. The different letters indicate significant statistical differences ($P < 0.05$, Turkey's HSD test).
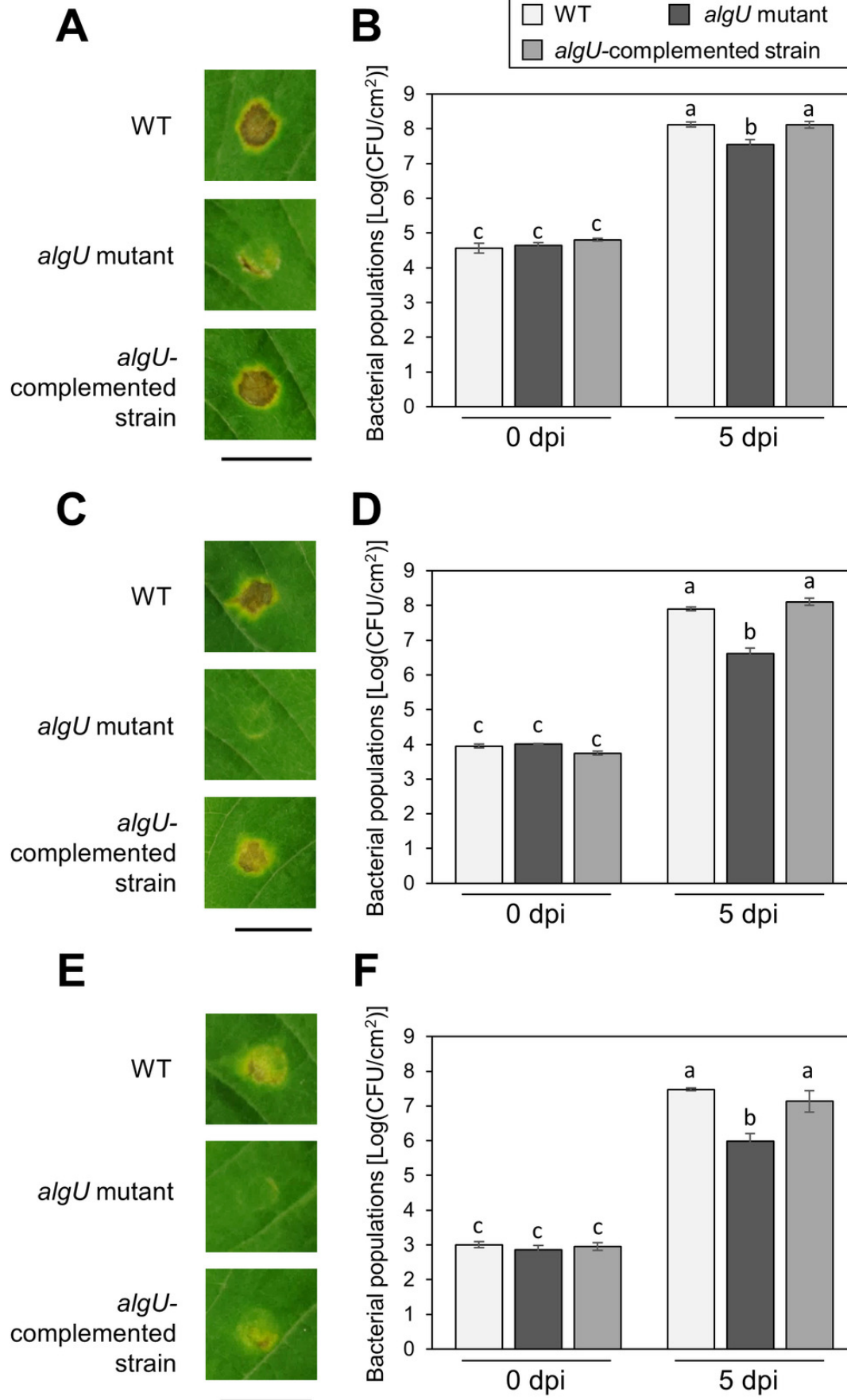
Figure 4

Gene expression profiles involved in the virulence of *Pseudomonas savastanoi* pv. *glycinea* (*Psg*) wild-type (WT) and *algU* mutant in liquid HSC broth.

Psg WT and *algU* mutant were grown in HSC broth for 3 and 48 h, adjusted to an OD_{600} of 0.1, and grown again in fresh HSC broth for 3 h. Gene expression was normalized using the housekeeping gene *Psg outer membrane lipoprotein I* (*oprI*) by real-time quantitative reverse transcription-polymerase chain reaction (RT-qPCR) with gene-specific primer sets (Supplementary Table S1). (A) *cmaA*, (B) *cfl*, (C) *corR*, (D) *hrpL*, (E) *fliC*, and (F) *algD*. Vertical bars indicate the standard error for three biological replicates. The different letters (a-c) indicate a significantly statistical difference ($P < 0.05$, Turkey's HSD test).
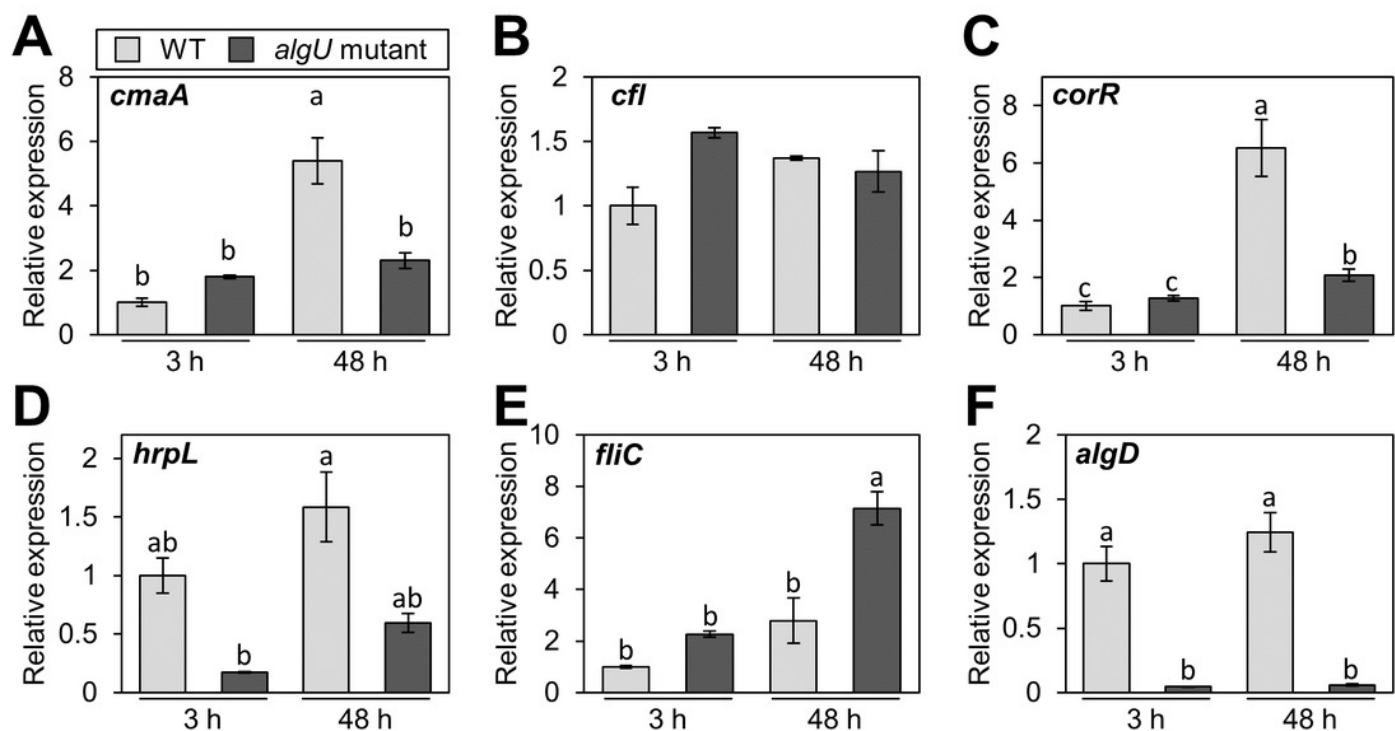
Figure 5

COR quantification of *Pseudomonas savastanoi* pv. *glycinea* (*Psg*) wild-type (WT), the *algU* mutant, and the *algU*-complemented strain.

(A) Observation of hypertrophy-inducting activity on potato tuber tissue inoculated with *Pseudomonas savastanoi* pv. *glycinea* (*Psg*) wild-type (WT), COR-defective mutants (*cmaA* and *cfa6*), the *algU* mutant, and the *algU*-complemented strain. Potato tuber discs were inoculated using toothpicks by placing the tips in the *Psg* WT, *cmaA*, *cfa6*, *algU* mutant, and the *algU*-complemented strain on a KB medium plate and then placing the toothpick on the potato tuber disc. Photographs were taken at 5 dpi. (B) COR quantification of *Pseudomonas savastanoi* pv. *glycinea* (*Psg*) wild-type (WT) and the *algU* mutant grown in liquid HS broth by HPLC. *Psg* WT, the *algU* mutant, and the *algU*-complemented strain were cultured in HSC broth for 7 days. HPLC analysis was conducted by a Shimadzu LC20A system equipped with a Symmetry C8 column. COR in the culture supernatant was identified, as compared with authentic COR as the standard. Vertical bars indicate the standard error for three biological replicates. Asterisks indicate a significant difference from WT in a *t* test (** $P < 0.01$). N.D. indicates not detected by HPLC.
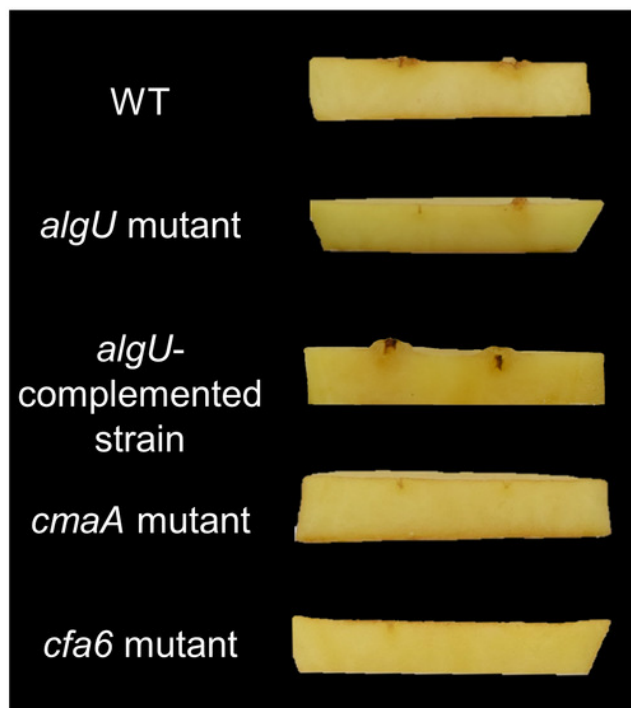
A **B**
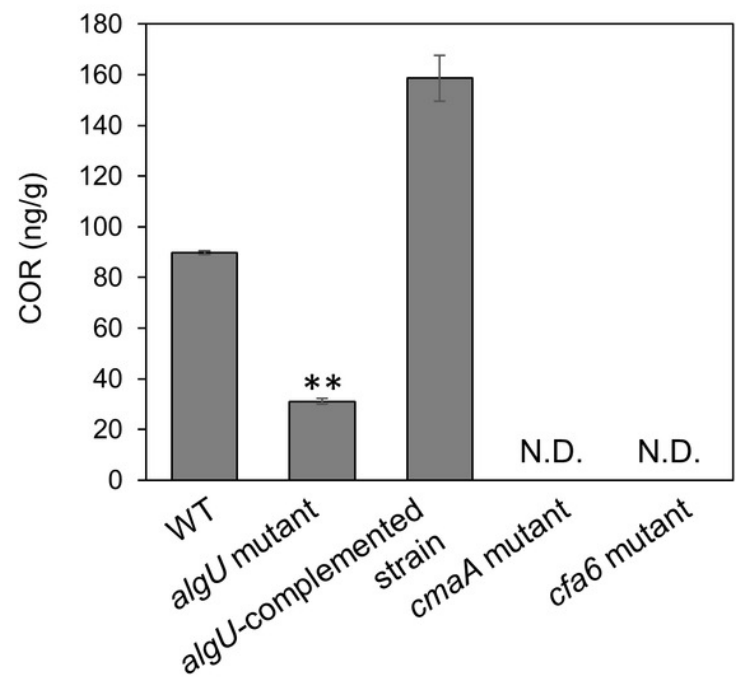
Figure 6

Biofilm biomass measurement of *Pseudomonas savastanoi* pv. *glycinea* (*Psg*) wild-type (WT) and the *algU* mutant with crystal violet (CV) grown in LB broth at 28°C for 24, 48, 72, and 96 h.

The biofilm eluted sample's absorbance was measured at OD_{595}. Vertical bars indicate the standard error for three biological replicates. Asterisks indicate a significant difference from WT in a *t* test (* $P < 0.05$, ** $P < 0.01$).